

Delta (δ) Ferrite Formation in the Welds of Aluminized 9Cr-1Mo Steels

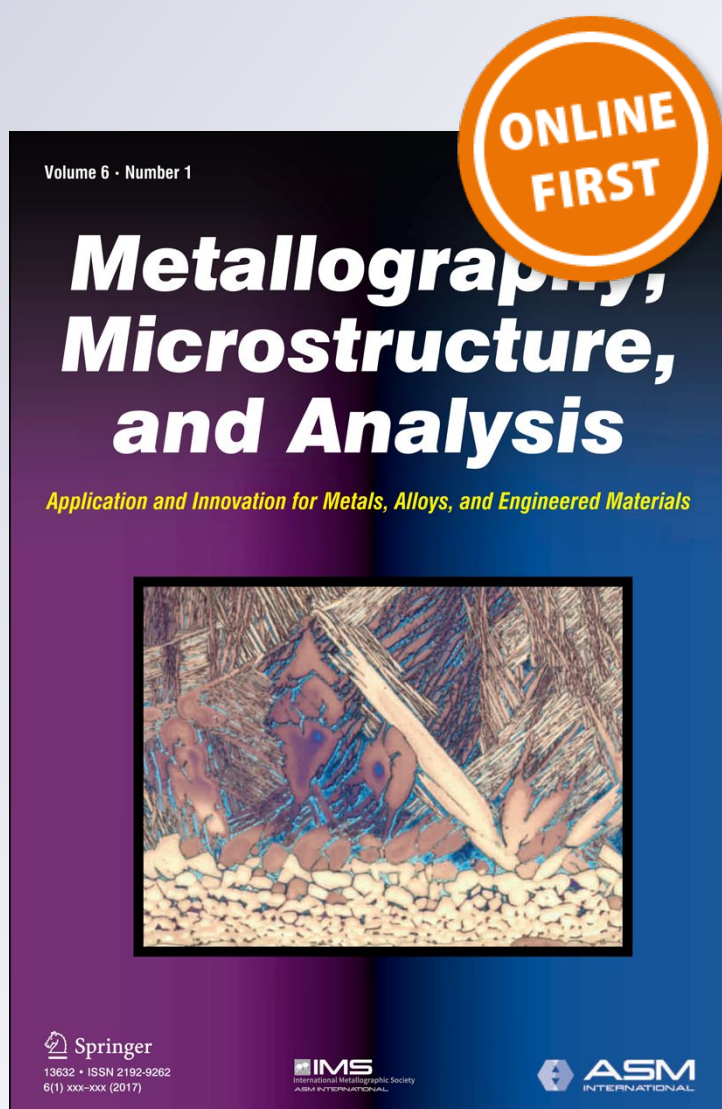
**A. B. Zala, N. I. Jamnapara,
V. J. Badheka, C. Sasmal, S. Sam &
M. Ranjan**

Metallography, Microstructure, and Analysis

Application and Innovation for Metals, Alloys, and Engineered Materials

ISSN 2192-9262

Metallogr. Microstruct. Anal.
DOI 10.1007/s13632-019-00528-1



Your article is protected by copyright and all rights are held exclusively by ASM International. This e-offprint is for personal use only and shall not be self-archived in electronic repositories. If you wish to self-archive your article, please use the accepted manuscript version for posting on your own website. You may further deposit the accepted manuscript version in any repository, provided it is only made publicly available 12 months after official publication or later and provided acknowledgement is given to the original source of publication and a link is inserted to the published article on Springer's website. The link must be accompanied by the following text: "The final publication is available at link.springer.com".



Delta (δ) Ferrite Formation in the Welds of Aluminized 9Cr-1Mo Steels

A. B. Zala^{1,2} · N. I. Jamnapara^{1,2} · V. J. Badheka³ · C. Sasmal¹ · S. Sam¹ · M. Ranjan^{1,2}Received: 26 July 2018 / Revised: 21 January 2019 / Accepted: 5 February 2019
© ASM International 2019

Abstract

Delta (δ) ferrite phase has several detrimental effects on mechanical properties such as toughness, creep, impact and ductility. It is necessary to examine δ -ferrite content in the weld zone of aluminized coated steels. This manuscript presents the investigation of δ -ferrite formation in the weld of aluminized P91 steels. The welds were prepared with different heat inputs by varying the weld speed at constant current by autogenous Tungsten Inert Gas (TIG) welding process. The concentration of Al in the weld zone may favor δ -ferrite formation during the welding as Al is a ferrite former. Hence, the weld zone prepared at maximum heat inputs was compared for both coated and bare P91 samples. Microstructures were examined and correlated with the temperatures and cooling curve measured during welding. The various empirical formulae such as Schneider, Schaeffler, Newhouse, and Kaltenhauser were used to predict the δ -ferrite formation based on the chemical composition of weld metal obtained with the help of spark emission spectroscopy. Among these, Kaltenhauser's equation is more accurate for aluminized coated P91 steels. X-ray diffraction, optical microscopy, scanning electron microscopy, and microhardness measurement were done to analyze and predict the shape and morphology of δ -ferrite for coated steel and bare P91 steels. The investigation indicates that higher heat input (~ 2.12 kJ/mm) for coated steel and Al concentration ($\sim 0.19\%$) in the weld zone caused the formation of δ -ferrites in various shapes such as polygonal and isolate islands and it has an average volume fraction of $\sim 5.09\%$. The average microhardness values were ~ 396 – 410 Hv for martensitic laths, while it was ~ 192 – 198 Hv for delta ferrite which is 52% lower.

Keywords δ -ferrite · Microstructure · Aluminized 9Cr steels · TIG welding

Introduction

The 9Cr-1Mo steels are firstly introduced by Oak Ridge National Lab for the petrochemical plant applications, subsequently incorporated in the ASTM specifications as P91 (ASTM 1986) [1]. Later on, these P91 steels are considered as a promising material as it offers superior creep and tensile properties, high thermal conductivity, low thermal expansion, good ductility, and high toughness. Due to this, it has numerous applications in nuclear power plants, turbine driven

systems, fast breeder reactors, and thermal power plants [2–4]. Moreover, to enhance the high-temperature oxidation resistance and corrosion resistance and to mitigate issues like tritium permeation, magneto-hydrodynamic drag, $\text{Al}_2\text{O}_3 + \text{FeAl}$ coatings have been reported as a keen solution especially for fusion nuclear applications [5–8]. The coating processes of aluminizing have been optimized microstructurally followed by several heat treatments like normalizing and plasma tempering [9–14]. However, the challenging issue associated with this coating process is the fabrication sequence. The presence of Al in the weld metal from the coated surface can cause the formation of delta ferrite as Al is a ferrite former [15]. Bertin et al. [16, 17] reported that an arc welding of Aluminium coated steel resulted in to delta ferrite formation in the welded joint and inferior the tensile strength. Briand et al. [18] determined the presence of aluminum ($> 2\%$) in weld pool, which gives rise to the form of delta ferrite and results in lower hardness in the weld zone. Delta ferrite formation may enhance solidification cracking, impair toughness due to notch sensitivity of the delta ferrite phase, and reduce the creep ductility at

✉ A. B. Zala
arun.zala@ipr.res.in; arunsinh54@gmail.com

¹ Institute for Plasma Research, Near Indira Bridge, Gandhinagar District, Bhat, Gujarat 382428, India

² Homi Bhabha National Institute, 2nd Floor, BARC Training School Complex, Anushaktinagar, Mumbai, Maharashtra 400094, India

³ Pandit Deendayal Petroleum University Raisan, Gandhinagar 382421, Gujarat, India

high temperature in 9–12% Cr metals and welds [19]. Wang et al. and Anderko et al. [20, 21] reported that the presence of delta ferrite deteriorates the impact properties and raises the DBTT of the martensitic stainless steel.

The formation of delta ferrite also depends on the heat input during the welding process. Arivazhagan et al. [22] have explained the emergence of delta ferrite due to high heat input during autogenous GTAW for reduced activation ferritic martensitic (RAFM) steels. The effect of heat input and cooling rate is also studied by Sam et al. [23], and delta ferrite was reported in the weld metal interface of RAFM steels because of the epitaxial growth from partially melted ferrite grains. These RAFM steel has been developed for fusion reactor applications with P91 steel as a surrogate material. δ -ferrite evolution during the welding of dissimilar P91-P92 steel weld joints has been reported by Pandey et al. [24, 25]. There is nevertheless a paucity of reliable data regarding the welding of coated steel and delta ferrite in the weld zone of aluminized P91 steel. Hence, it is essential to examine the presence of delta ferrite along with the aluminum concentration in the weld zone as its presence will affect the mechanical properties.

This experimental work is carried out to investigate the delta ferrite formation in the weld metal of aluminized coated steel. The bead-on-plate trials were conducted on aluminized and bare P91 steel by varying the heat inputs to analyze the effect of heat input on the emergence of delta ferrite. The weld prepared at 100 mm/min and 200 A current for coated steel was having maximum heat input. X-ray diffraction of this weld metal revealed the presence of delta ferrite. In addition, to predict the delta ferrite theoretically, various empirical formulae have been reported and co-related with microstructures and Vickers microhardness indentations were taken within the delta ferrite region.

Experimental Work

Aluminizing and Welding

P91 steel samples as per composition reported in ASTM A387 Grade 91 standard with 9 wt.% Cr and 1 wt.% Mo as major alloying elements were cut to size 75 mm \times 25 mm \times 5 mm. The chemical compositions of other elements are mentioned in Table 1. The samples were polished and subjected to ultrasonic cleaning for 10 min. After that, hot dipping was done in a molten bath of 93% Al-7% Si at \sim 730 $^{\circ}$ C for 30 s and heat treatments were carried out as reported by Jamnapara et al. [9, 11, 14]. The weld beads of aluminized samples were

prepared by gas tungsten arc welding (GTAW) power source (Panasonic) having a capacity of 200 A with 25% duty cycle and customized special purpose machine for torch movement at predefined weld speed. The heat input for the weld was altered by varying the travel speed at the same current. The welding current for both coated and bare P91 materials was kept constant, i.e., 200 A (2.12 kJ/mm). The other parameters are mentioned in Table 2 which were considered for the welding trials. These all parameters were fixed after several experiments and investigation of their weld bead's size and shape. To observe the cooling rate and to correlate the peak temperatures during the welding with microstructures, contact thermocouples (K-type) were used. The location was 10 mm away from the centerline of weld bead for both coated and bare P91 samples. The same trials were conducted four times to ensure the repeatability.

Characterization of the Weld

The cross sections of weld bead prepared from coated and bare P91 steel were subjected for X-ray diffraction. The XRD was conducted to identify the phases in the weld with D8 discover model of Bruker with Cu K α radiation ($\lambda = 1.5406 \text{ \AA}$) in Bragg–Brentano geometry. The 2θ range was 20° – 80° at 0.05 step/size increment and 0.5 s/step time. The metallographic specimens were prepared by polishing, and the mirror-finish surface was etched as per the standard practice mentioned in ASTM E 407-99 by swabbing with Villella's solution (Picric acid 10 g + HCL 5 ml + methanol 100 ml). The microstructures were examined with SDM 210 (Make: SEIWA JAPAN) optical microscope. Along with the welded cross sections, the microstructure of as-received

Table 2 GTAW parameters for coated and bare P91 samples

| | |
|---------------------|-----------------------------|
| Welding current | 200, A |
| Creator current | 160, A |
| Travel speed | 100,125,150, mm/min |
| Electrode type | Tungsten (2% thoriated) |
| Electrode diameter | 2.9, mm |
| Electrode angle | 18–20 (blunt ground at tip) |
| Arc gap | 2–3, mm |
| Gas flow rate | 10–12, l/min |
| Welding position | 1 G (flat) |
| Electrode extension | 5–6, mm |
| Nozzle diameter | 8, mm |

Table 1 Chemical composition of ASTM A 387 Gr91 steel (P91) in wt.%

| Elements | | | | | | | | | | | | | |
|----------|------|------|------|------|-------|------|------|------|------|------|------|------|---------|
| C | Cr | Mo | Si | Mn | Nb | V | Al | S | P | Cu | Ni | N | Fe |
| 0.09 | 9.30 | 0.88 | 0.20 | 0.45 | 0.088 | 0.20 | 0.04 | 0.01 | 0.02 | 0.10 | 0.20 | 0.07 | Balance |

P91 steel was investigated. The normalizing treatment has been carried out in the range of 1040–1090 °C for soaking of 0.5 h and cooled in air, and the tempering process was done at ~780–785 °C with a holding time of 1 h followed by cooling in air for as-received P91 steel. The scanning electron microscopy (SEM-Model: Carl Zeiss, Supplier: VP Merlin, Germany) was done to identify the delta ferrite within the weld zone. The microhardness measurement was done to confirm the delta ferrite phase at 50-g load with dwell time of 20 s. As Sam et al. [23] reported, similarly the microhardness spots were taken in delta ferrite region and in maternities lath colony as delta ferrite is softer compared to martensite.

Results and Discussion

Effect of Heat Input

As mentioned in the experimental work, the weld speed was varied (100,125,150 mm/min) along with the constant current 200 A for both coated and bare P91. However, the heat input measured for the aluminized P91 steel was higher (2.12 kJ/mm) compared to the bare samples (1.44 kJ/mm) at same current and same weld speed. The coating contains oxides (Al_2O_3) at the surface which interacts with the arc during the welding. During the arc interaction at the time of welding, electrons from the electrode interact with the coated layer of the substrate. As Al_2O_3 oxide layer has good insulation property, the electron does not get the free path to travel on the surface. Due to this, arc gets constrict and temperature of weld pool for coated steel would be higher at same welding parameters. As a result, the heat input for the coated steel will be higher. This effect is known as insulating effect reported by Vilarinho et al. [26]. Hence, to investigate the effect of heat input X-ray diffraction was done at cross sections of welds. Figure 1 shows diffractograms of weld zone where Fig. 1a indicates peaks for weld metal of bare P91 steel, while Fig. 1b is for coated weld sample. In Fig. 1a, peaks at $2\theta=45.07^\circ$ and 65.64° corresponding to the plane (110) and (200) reveal α -ferrite phase as per the ICDD (International Center for Diffraction Data) card no. 01-076-6587. However, for the weld of coated steel, the presence of delta ferrite was observed because of the peak indication at $2\theta=43.6285^\circ$. ICDD card no. 01-089-4186 confirms the peak of delta ferrite with the plane of (110) though the intensity of peak is low.

While welding was done, the peak temperature was measured 10 mm away from the centerline of the weld. It was approximately 1120 °C for the coated steel, while it is 670 °C for bare P91 steel. The time vs temperature plot is shown in Fig. 2. Under the equilibrium condition, liquid metal solidifies as delta ferrite and the transformation of

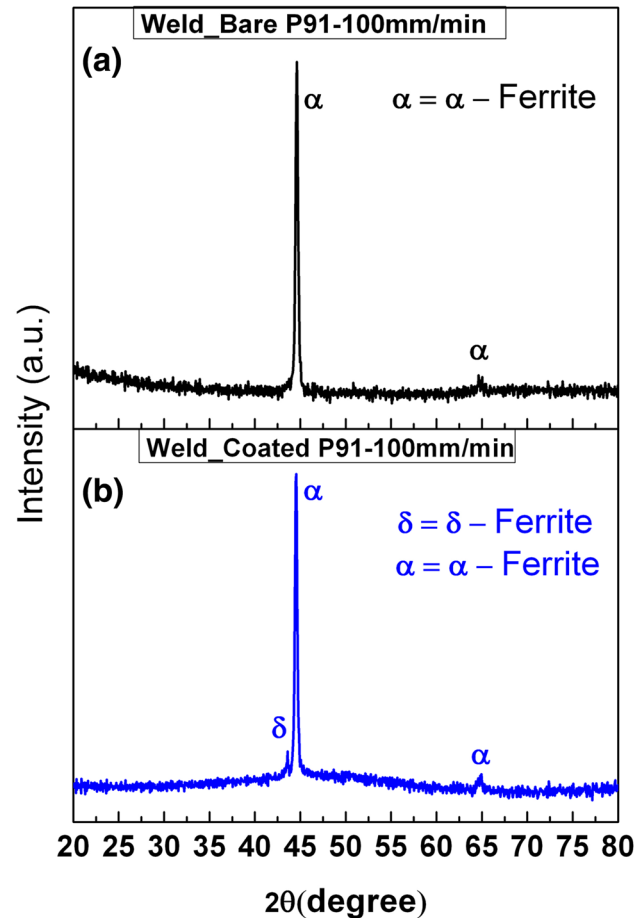


Fig. 1 X-ray diffraction plot of weld metal prepared at 100 mm/min weld speed and 200 A current for coated and bare P91 steels

delta ferrite into austenite crystals starts at around 1300 °C and ends at around 1200 °C [23]. However, this equilibrium transformation is not possible during weld cooling cycle. The higher cooling rate in weld zone causes more delta ferrite formation [19], and as the delta ferrite will not get adequate time to transform to austenite, it will remain within the weld zone at ambient temperature. The figure indicates that the cooling rate was higher for the coated P91 steel. Hence, the results from XRD and time vs temperature plot increase the likely formation of delta ferrite.

Delta Ferrite Prediction in Welds

To predict the δ -ferrite in the weld zone, several empirical formulae have been reported. The equation describes the difference between the weighted effects for the ferrite and austenite forming elements, i.e., the chromium and nickel equivalent values. Authors [19, 22, 23, 27–29] have quoted empirical formulas such as Schaeffler, Schneider, Kaltenhauser, and Newhouse. Each formula has been modified

according to various major alloying elements and with the help of chemical composition; the formation of delta ferrite can be predicted. Sam et al. [23] have considered Newhouse formula as their investigation was with regard to reduced activation ferritic martensitic (RAFM) steels where elements such as W, Nb, and V were major alloying elements. Arivazhagan et al. [22, 29] utilized Schneider equation and modified it, as the Ta element was not taken into the account though it is a ferrite stabilizer and was a principal alloying element in their case. Pandey et al. [30, 31] reported Schneider equation and explained the effect of delta ferrite on impact toughness for the dissimilar weld joints of 9Cr steels.

Hence, the spectroscopy was done at the center of the weld for both coated and bare 9Cr-1Mo samples, so the values can be a substitute to the respective formulae. The chemical composition of different elements is shown in

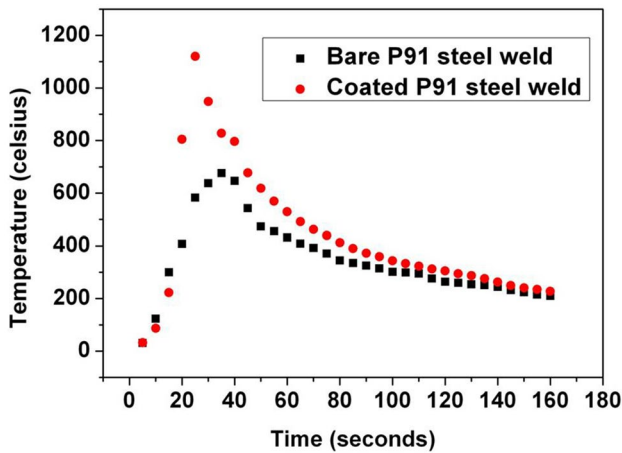


Fig. 2 Time vs temperature comparison for coated and bare P91 steels for the weld prepared at 100 mm/min weld speed and 200 A current

Table 3. The material 9Cr-1Mo steel has 0.04% Al in as-received condition as shown in Table 1. However, for the coated weld Al concentration was increased from 0.04% to 0.19% and Al plays a dominant role in delta ferrite formation as it is a ferrite stabilizer [15]. So, from different equations, Kaltenhauser formula was more suitable to improve the accuracy as it increases the weighted effect of aluminum and it has been reported for 9Cr steels [19, 27, 28].

The Kaltenhauser equation is mentioned below.

$$Cr_{eq} = Cr + 6Si + 4Mo + 8Ti + 2Al + 4Nb$$

$$Ni_{eq} = 2Mn + 4Ni + 40(N + C)$$

where Cr_{eq} is 'chromium equivalent' and Ni_{eq} is 'Nickel equivalent.' The difference between Cr_{eq} and Ni_{eq} values is known as ferrite factor. The calculated ferrite factor and delta ferrite prediction from Kaltenhauser and other empirical formulae are shown in Table 4. As referred by [22, 23, 29], if the ferrite factor ($Cr_{eq} - Ni_{eq}$) is above 10, then there is a possibility of delta ferrite formation in weld pool.

Microstructure

The results from various empirical formulas indicate that the delta ferrite is expected within the weld metal of coated steels. Hence, the microstructure of P91 is analyzed through optical microscopy in as-received condition and then compared with the microstructures of weld metal for coated and un-coated welds. The material considered for the experimental work was undergone heat treatments such as normalizing and tempering. The normalizing treatment was done at 1040–1090 °C for half an hour, and tempering was done at ~780 °C with holding time of 1 h followed by cooling in air. Figure 3 illustrates the tempered martensite

Table 3 Emission spectroscopy results of weld metal for coated weld and un-coated (bare) welds

| Elements (spectroscopy) | C | Cr | Mo | Si | V | Mn | Al | Nb | Ti | N | Ni | Cu | Fe |
|-------------------------|-------|-------|-------|-------|-------|-------|-------|-------|-------|-------|-------|-------|---------|
| Coated weld, wt. % | 0.14 | 8.70 | 0.95 | 0.22 | 0.21 | 0.40 | 0.19 | 0.07 | 0.04 | 0.06 | 0.31 | 0.05 | Balance |
| Un-coated weld, wt. % | 0.21 | 8.59 | 0.98 | 0.20 | 0.21 | 0.41 | 0.03 | 0.07 | 0.04 | 0.04 | 0.30 | 0.07 | Balance |
| SD, ± | 0.006 | 0.081 | 0.001 | 0.018 | 0.001 | 0.010 | 0.001 | 0.008 | 0.001 | 0.006 | 0.017 | 0.013 | 0.005 |

Table 4 Ferrite factor prediction for 9Cr-1Mo steel in various conditions from various formulae

| | | Schaeffler | Schneider | Kaltenhauser | Newhouse |
|----------------|--|------------|-----------|--------------|----------|
| As received | Ferrite factor ($Cr_{eq} - Ni_{eq}$) | 5.92 | 7.67 | 6.88 | 6.95 |
| | Delta ferrite prediction | No | No | No | No |
| Coated Weld | Ferrite factor ($Cr_{eq} - Ni_{eq}$) | 5.92 | 5.64 | 12.75 | 9.75 |
| | Delta ferrite prediction | No | No | May be | No |
| Un-coated weld | Ferrite factor ($Cr_{eq} - Ni_{eq}$) | 3.29 | 5.80 | 4.36 | 7.38 |
| | Delta ferrite prediction | No | No | No | No |

microstructure of P91 steel in as-received condition after both the heat treatments. Optical image of weld metal for un-coated steel is shown in Fig. 4. Weld metal has fully martensitic laths, and prior austenite grain boundaries are

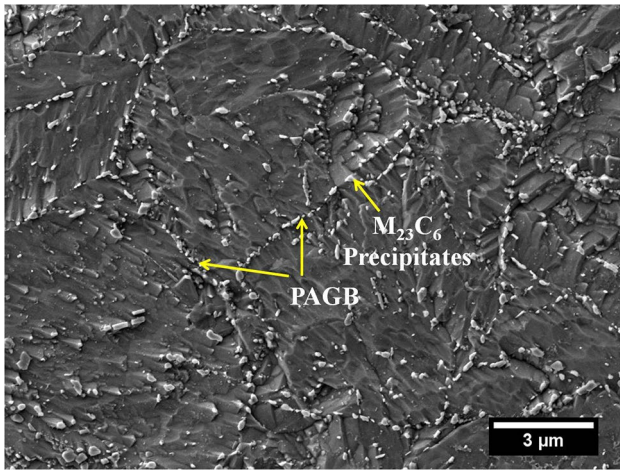


Fig. 3 SE image of P91 steel's microstructure in as-received condition

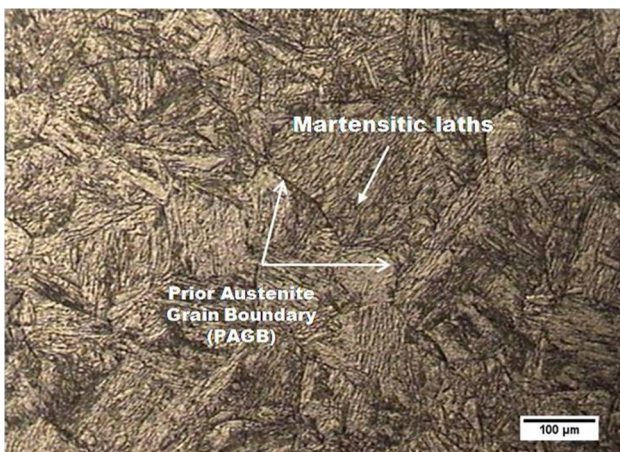
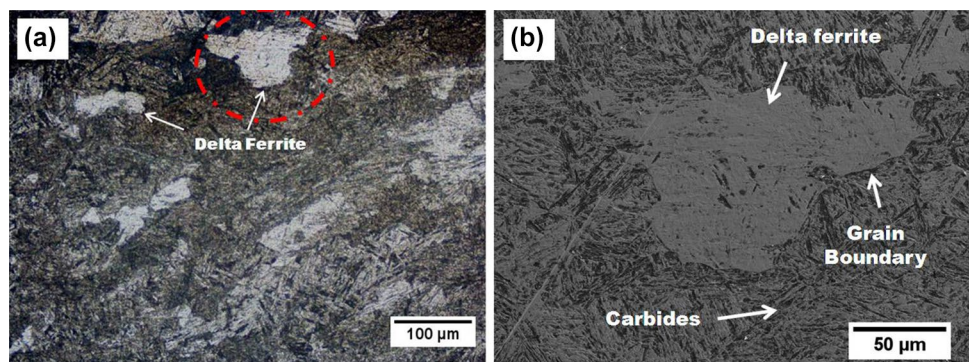


Fig. 4 Weld metal's microstructure of bare P91 steel prepared at 100 mm/min weld speed and 200 A current

Fig. 5 Weld metal's microstructure of coated P91 prepared at 100 mm/min weld speed and 200 A current. The encircled part in (a) (optical image) is highlighted as (b) (SE image)



identical. The weld metal is free from delta ferrite, which supports the prediction mentioned in Table 4 derived from empirical formulas.

Figure 5 shows optical as well as SE image of weld metal in as-weld condition produced through autogenous TIG welding process at 2.12 kJ/mm heat input (weld current 200 A, weld speed 100 mm/min). The morphology of weld metal indicates the presence of delta ferrite. To investigate the same, SE image (Fig. 5b) was taken at an encircled area in Fig. 5a. The delta ferrite is free from carbides as reported by Arivazhagan et al. [22]. SE image (Fig. 5b) shows a delta ferrite region where carbides are completely absent. The prediction of delta ferrite (ferrite factor) through empirical formulae has also supported the formation of delta ferrite. Delta ferrite in polygonal shape and island of delta ferrite in a matrix of tempered martensite have been reported [19, 27]. Similar kind of polygonal shape of delta ferrite is observed and shown in Fig. 6a, while Fig. 6b illustrates island of delta ferrite in martensite matrix structure. In addition, these phases were higher at grain boundaries, while the interior of grain showed less delta ferrite phase. This is due to more energy available at the grain boundary than at the grain interior region and hence the variation in quantity of delta ferrite [22]. The volume fraction of delta ferrite was analyzed through image J software within weld zone. The amount of delta ferrite in the weld zone was noticed ~5.03% which is a bit of concern as the mechanical properties may get deteriorate.

Microhardness of Delta Ferrite

Microhardness was measured to support the prediction of delta ferrite formation. The measurements were done at the load of 0.05 kg at a dwell time of 20 s at different delta ferrite locations. As explained, the delta ferrites are free from carbides; hence, certainly in the absence of carbides and precipitates the hardness value would be lower compared to martensite. Sam et al. [23] have reported that the delta ferrite would be leaner in carbon during the subsequent transformation of delta ferrite to austenite and austenite to martensite

Fig. 6 Polygonal delta ferrite and (b) island of delta ferrite in matrix of tempered martensite observed at prepared at 100 mm/min weld speed and 200 A current

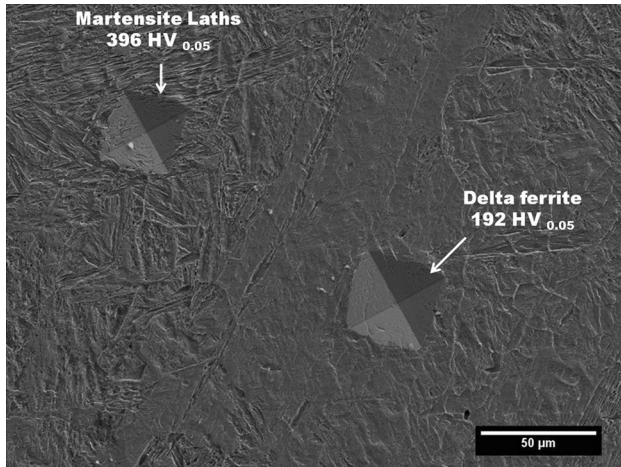
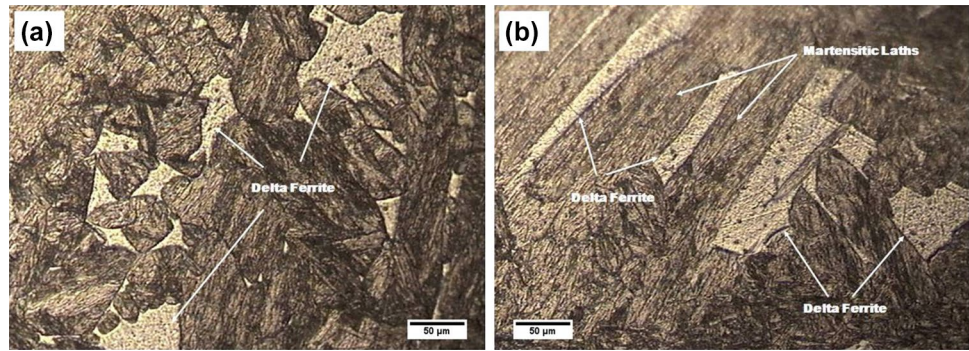


Fig. 7 SE image indicating micro-Vicker hardness indentations at 0.05 kg load and values for phases in the weld zone prepared at 100 mm/min weld speed and 200 A current

and hardness would be lower of delta ferrite at same load. To confirm the delta ferrite, indentations were taken and the values were $\sim 195 \pm 5$ HV for reduced activation ferritic martensitic (RAFM) steels [23]. Pandey et al. [31] have also measured the microhardness in delta ferrite region and reported different values such as 190 ± 10 HV, 198 ± 10 HV. SE image which includes microhardness indentation in martensite region and delta ferrite is shown in Fig. 7. The phase which consists of carbides, i.e., martensite, has $\sim 396 \pm 5$ HV_{0.05}. Delta ferrite is comparatively softer, and the value was recorded roughly 192 ± 5 HV_{0.05}.

Conclusions

From the results presented above, it is clear that though the probability of having delta ferrite in the weld metal, based on the chemical composition, is very low, the weld metal prepared at 100 mm/min and 200 A weld current for aluminized coated steel does contain delta ferrite.

Further, variations in volume fraction and morphology of the d-ferrite are observed within the fusion zone and also with respect to changes in welding parameters. The conclusions for this investigation are mentioned below.

- Al concentration in the weld zone may cause the formation of delta ferrite as Al is acting as a ferrite former.
- A good co-relation can be established between a theoretical prediction of delta ferrite and volume fraction of delta ferrite by microscopy investigation. From various empirical formulae, Kaltenhauser's equation is more accurate to predict the delta ferrite as it has a higher Al weight percentage. In addition, the spectroscopy results of weld metal revealed $\sim 0.19\%$ Al.
- One of the possible reasons for the formation of delta ferrite could be high heat input. Alumina coating at the surface constricts the arc, and due to that heat input was higher for coated steels. So, the volume fraction observed of delta ferrite was $\sim 5.09\%$ at 2.12 kJ/mm (100 mm/min weld speed, 200 A current) for coated steels. The X-ray diffraction analysis also revealed the presence of delta ferrite phase.
- The delta ferrite appearance was in polygonal shape and was distinguished at prior austenitic grain boundaries. Isolate island of delta ferrite in a martensite matrix was also noticed.
- The delta ferrites were free from carbides, and subsequently, the hardness was low (~ 192 HV) compared to martensite which has 396 HV.

This investigation can be further continued to examine the effect of pre-heating on cooling rate during welding and subsequently on the formation of delta ferrite. Another major aspect is to analyze the effect of delta ferrite volume fraction on tensile and impact properties of weld joint.

Acknowledgement The authors sincerely acknowledge the experimental support of Mr. Janik Malaviya and Mr. Subrat Das (IPR) to conduct the hot dipping process for coating and for the heat treatments. The authors are thankful to Mr. K.P. Singh (IPR) for providing guidance with regard to microscopy. The support from Mr. Yogendra Singh (IPR) is also appreciated for microhardness measurements.

References

1. C. Coussement, A. Dhooge, M. de Witte, R. Dobbelaere, E. van der Donckt, High temperature properties of improved 9% Cr steel weldments. *Int. J. Press. Vessels Pip.* **45**(2), 163–178 (1991)
2. F. Abe, Alloy Design of Advances Ferritic Steels for 659 C USC Boilers, in *Conf. Proc. Advanced Heat Resistant Steel for Power Generation. San Sebastian. Spain. University Press, Cambridge. UK*, (1998), pp. 84–87
3. R.L. Klueh, D.R. Harries, *High Chromium Ferritic and Martensitic Steels for Nuclear Applications* (ASTM International, West Conshohocken, PA, 2001)
4. S. Mannan, S. Chetal, B. Raj, S. Bhoje, Selection of materials for prototype fast breeder reactor. *Trans.-Indian Inst. Metals* **56**(2), 155–178 (2003)
5. H. Yang, Q. Zhan, W. Zhao, X. Yuan, Y. Hu, Z. Han, Study of an iron-aluminide and alumina tritium barrier coating. *J. Nucl. Mater.* **417**(1), 1237–1240 (2011)
6. Y. Ueki, T. Kunugi, N.B. Morley, M.A. Abdou, Electrical insulation test of alumina coating fabricated by sol–gel method in molten PbLi pool. *Fusion Eng. Des.* **85**(10), 1824–1828 (2010)
7. W. Krauss, J. Konys, N. Holstein, H. Zimmermann, Al-based anti-corrosion and T-permeation barrier development for future DEMO blankets. *J. Nucl. Mater.* **417**(1), 1233–1236 (2011)
8. A. Aiello, I. Ricipito, G. Benamati, A. Ciampichetti, Qualification of tritium permeation barriers in liquid Pb–17Li. *Fusion Eng. Des.* **69**(1), 245–252 (2003)
9. N. Jamnapara, D. Avtani, N. Chauhan, P. Raole, S. Mukherjee, A. Khanna, Effect of Si on morphology of alumina scales. *Surf. Eng.* **28**(9), 693–699 (2012)
10. N. Jamnapara, S. Frangini, J. Alphonsa, N. Chauhan, S. Mukherjee, Comparative analysis of insulating properties of plasma and thermally grown alumina films on electrospark aluminide coated 9Cr steels. *Surf. Coat. Technol.* **266**, 146–150 (2015)
11. N. Jamnapara, S. Mukherjee, A. Khanna, Phase transformation of alumina coating by plasma assisted tempering of aluminized P91 steels. *J. Nucl. Mater.* **464**, 73–79 (2015)
12. N. Jamnapara, V. Nayak, D. Avtani, N. Chauhan, D. Panda, S. Gupta, K. Kalaria, N. Vaghela, S. Mukherjee, A. Khanna, Al₂O₃ films grown by glow discharge plasma aluminising. *Surf. Eng.* **30**(7), 467–474 (2014)
13. N.I. Jamnapara, S. Frangini, D. Avtani, V. Nayak, N. Chauhan, G. Jhala, S. Mukherjee, A. Khanna, Microstructural studies of electrospark deposited aluminide coatings on 9Cr steels. *Surf. Eng.* **28**(9), 700–704 (2012)
14. N.I. Jamnapara, A.S. Sree, E.R. Kumar, S. Mukherjee, A. Khanna, Compatibility study of plasma grown alumina coating with Pb–17Li under static conditions. *J. Nucl. Mater.* **455**(1), 612–617 (2014)
15. A. Mein, G. Fournalis, D. Crowther, P. Evans, The influence of aluminium on the ferrite formation and microstructural development in hot rolled dual-phase steel. *Mater. Charact.* **64**, 69–78 (2012)
16. P. Bertin, O. Dubet, S. Gadrey, F. Richard, *Method For Arc-Welding Aluminum-Coated Metal Parts Using An Inert Gas Containing Nitrogen*, ed., Google Patents, 2011
17. P. Bertin, O. Dubet, S. Gadrey, F. Richard, *Method For Arc-Welding Aluminum-Coated Metal Parts Using Oxidizing Gas*, ed., Google Patents, 2011
18. F. Briand, O. Dubet, *Hybrid Arc/Laser-Welding Method For Aluminized Steel Part Using A Gas Including Nitrogen And/Or Oxygen*, ed., Google Patents, 2011
19. J. Onoro, Martensite microstructure of 9–12% Cr steels weld metals. *J. Mater. Process. Technol.* **180**(1), 137–142 (2006)
20. P. Wang, S. Lu, N. Xiao, D. Li, Y. Li, Effect of delta ferrite on impact properties of low carbon 13Cr–4Ni martensitic stainless steel. *Mater. Sci. Eng. A* **527**(13), 3210–3216 (2010)
21. K. Anderko, L. Schäfer, E. Materna-Morris, Effect of the δ -ferrite phase on the impact, properties of martensitic chromium steels. *J. Nucl. Mater.* **179**, 492–495 (1991)
22. B. Arivazhagan, G. Srinivasan, S. Albert, A. Bhaduri, A study on influence of heat input variation on microstructure of reduced activation ferritic martensitic steel weld metal produced by GTAW process. *Fusion Eng. Des.* **86**(2), 192–197 (2011)
23. S. Sam, C. Das, V. Ramasubbu, S. Albert, A. Bhaduri, T. Jayakumar, E.R. Kumar, Delta ferrite in the weld metal of reduced activation ferritic martensitic steel. *J. Nucl. Mater.* **455**(1), 343–348 (2014)
24. C. Pandey, M.M. Mahapatra, P. Kumar, N. Saini, Dissimilar joining of CFEF steels using autogenous tungsten-inert gas welding and gas tungsten arc welding and their effect on δ -ferrite evolution and mechanical properties. *J. Manuf. Process.* **31**, 247–259 (2018)
25. C. Pandey, M.M. Mahapatra, P. Kumar, N. Saini, Comparative study of autogenous tungsten inert gas welding and tungsten arc welding with filler wire for dissimilar P91 and P92 steel weld joint. *Mater. Sci. Eng. A* **712**, 720–737 (2018)
26. L.O. Vilarinho, V. Kumar, B. Lucas, S. Raghunathan, in *JOM-15-Fifteenth International Conference on the Joining of Materials and 6th International Conference on Education in Welding (ICEW 6)*, Helsingor, Denmark (2009)
27. J. Onoro, Weld metal microstructure analysis of 9–12%Cr steels. *Int. J. Press. Vessels Pip.* **83**(7), 540–545 (2006)
28. C. Pandey, A. Giri, M. Mahapatra, Evolution of phases in P91 steel in various heat treatment conditions and their effect on microstructure stability and mechanical properties. *Mater. Sci. Eng. A* **664**, 58–74 (2016)
29. B. Arivazhagan, M. Vasudevan, A comparative study on the effect of GTAW processes on the microstructure and mechanical properties of P91 steel weld joints. *J. Manuf. Process.* **16**(2), 305–311 (2014)
30. C. Pandey, M.M. Mahapatra, P. Kumar, N. Saini, Autogenous tungsten inert gas and gas tungsten arc with filler welding of dissimilar P91 and P92 steels. *J. Press. Vessel Technol.* **140**(2), 021407 (2018)
31. C. Pandey, M.M. Mahapatra, P. Kumar, N. Saini, J.G. Thakre, R. Vidyarthi, H. Narang, A brief study on δ -ferrite evolution in dissimilar P91 and P92 steel weld joint and their effect on mechanical properties. *Arch. Civil Mech. Eng.* **18**(3), 713–722 (2018)

Publisher's Note Springer Nature remains neutral with regard to jurisdictional claims in published maps and institutional affiliations.